

TAHER AZDAST, AMIR HOSSEIN BEHRAVESH¹⁾, KIUMARS MAZAHERI,
MOHAMMAD MEHDI DARVISHI

Tarbiat Modares University
Department of Mechanical Engineering
Tehran, Iran P. O. Box: 14115-143

Numerical simulation and experimental validation of residual stress induced constrained shrinkage of injection molded parts

Summary — In this paper a numerical analysis of in-mold constrained shrinkage of injection molded parts is presented, considering the residual stresses produced during the packing and cooling stages. Residual stresses are the main reasons of shrinkage and warpage of the injected parts. In regards to the viscoelastic characteristics of polymeric materials, mold constraints have noticeable effects on the final dimensions of the molded parts. A numerical analysis was developed and experimentally examined for constrained shrinkage using a case study: a plate containing the holes (as constraints). The results indicated a good agreement between the numerical solution and the experimental data.

Key words: injection molding, shrinkage, mold constraints, residual stress, cooling time.

SYMULACJA NUMERYCZNA I WERYFIKACJA DOŚWIADCZALNA WYMUSZONEGO SKURCZU WYPRASEK WTRYSKOWYCH JAKO WYNIK ODDZIAŁYWANIA NAPRĘŻEŃ WŁASNYCH

Streszczenie — Przedstawiono podstawy analizy numerycznej wymienionego w tytule zagadnienia w odniesieniu do skurczu na etapach docisku i chłodzenia w formie. Naprężenia własne stanowią główną przyczynę skurczu i odkształcania kształtek. Na końcowe ich wymiary wyraźny wpływ wywierają przeszkody w gnieździe formy wtryskowej. Wnioski wynikające z obliczeń symulacyjnych (rys. 4 i 6) porównano z wynikami doświadczalnymi otrzymanymi w badaniach z zastosowaniem kształtki o specjalnej konstrukcji (rys. 3) wykonanej z terpolimeru akrylonitryl/butadien/styren, uzyskując dobrą zgodność (rys. 7).

Słowa kluczowe: wtryskiwanie, skurcz, ograniczenia w formie, naprężenie własne, czas chłodzenia.

Injection molding is one of the most versatile production techniques of plastic parts manufacturing. In this process, polymeric melt is injected through a runner and a gate system into the mold cavity. The melt is then packed under a high pressure, during which the shrinkage is compensated to some extent, and then cooled until the part is solidified and is strong enough to be ejected. Residual stresses are usually developed during solidification in the postfilling stage. The stresses can be either flow-induced or thermal induced. However, in absolute values, the flow-induced stresses are usually one order of magnitude smaller than the thermal stresses [1].

Shrinkage, in molded plastic parts, can be affected by process parameters, part shape and mold design. Prediction of shrinkage is of great importance in design stage, and hence, understanding this inter-relationship assist designers in designing molds with less corrections. It is well known that processing parameters such as holding pressure, holding time, melt temperature, mold temperature, and part thickness have effects of certain de-

gree on final shrinkage. Besides, part design could have noticeable effect on shrinkage where constraints are involved. Although it is well known that cooling time influences the final shrinkage of the constrained dimensions, it can be still a subject of research interest. The effect is due to inter-relationship among viscoelastic characteristics of material, cooling time, and final part dimensions or shrinkage.

A numerical simulation of injection molding process can provide useful information to determine the appropriate processing conditions that could control the quality of the molded parts. Also the effects of material properties on the constrained shrinkage (here, viscoelastic parameters) can be investigated.

BACKGROUND

Extensive research was initiated by Williams and Pa-coast [2] to study the effects of processing parameters, mold and part design on shrinkage of various thermoplastics. Further study to analyze the effects of processing parameters on shrinkage was conducted by Mamat *et al.* [3]. They showed that holding pressure is the most

^{*)} Author to correspondence; P.O.Box 14115-143, Tehran, Iran; amirhb@modares.ac.ir

important process parameter affecting shrinkage. Their study further verified that the local pressure is directly correlated with the local shrinkage variation along the flow path.

Similar results were also reported by Leo and Cuveliez [4]. They studied the effect of gate thickness on dimensional accuracy of a part of rectangular shape.

Young [5], by developing a process simulation tool for an injection compression molding, demonstrated that a two-stage compression reduced pressure gradient in the cavity and caused low shrinkage.

Chang *et al.* [6] applied a finite volume algorithm to study the cooling behavior and thermal shrinkage of a molded compact disc. Further study to predict the effects of processing parameters on shrinkage was conducted by Xu and Kazmer [7] and Pontes [8].

Peng *et al.* [9] presented a numerical result for prediction of constrained warpage at the in-mold stage of a molded part. Their technique proved improvement in the accuracy of warpage analysis for complex geometry, but not indicating a detail description of the procedure.

Postawa [10] experimentally investigated the effects of mold temperature, injection temperature, clamping pressure, cooling time and injection speed on the longitudinal shrinkage, perpendicular shrinkage and weights of the injection molded parts made of semi-crystalline polyoxymethylene and amorphous polystyrene. His results showed that, to control the shrinkage value and molding weight in the industrial practice, it was the most advantageous to change the clamping pressure as essential easy-to-change parameter.

Chen *et al.* [11] investigated the feasibility of integrating simulation of mold flow for warpage of lens to estimate the shrinkage error in IM process with compensation of shrinkage error of lens for improving the efficiency of mold design for aspheric lens. They used Taguchi method to run experimental design for identifying the significant factors among injection parameters leading to minimum Z-axis deformation. Their results showed that the mold temperature was the most significant factor affecting the warpage.

Kowalska [12] simulated contraction in volume and strain of moldings made of isotactic polypropylene "Malen P" type J-400 prepared by injection molding using of the "Moldflow Plastics Insight ver. 4.1" software. She applied relations between pressure, specific volume and temperature (P-V-T) obtained in various cooling conditions. Results confirm the significant influence of P-V-T data used in the process simulation.

Boitout *et al.* [13] presented a method to calculate residual stresses in injection molding process using a 2-D description of geometry. They assumed that the polymer follows an elastic behavior. They also pointed out the influence of melt pressure and mold deformation on the residual stress distribution in a polystyrene square plaque.

Zoetelife *et al.* [1] numerically investigated the influence of holding stage on the distribution of the residual

thermal stress. During the holding stage in injection molding, when extra molten polymer is added to the mold to compensate the shrinkage, tensile stresses may develop at the surface, induced by the pressure during solidification. Their numerical and experimental results for two different amorphous polymers (ABS and PS) in the square plates forms were compared considering a linear viscoelastic constitutive law.

Choi and Im [14] carried out a numerical analysis of shrinkage and warpage in consideration of the residual stresses using a thermo-rheologically simple viscoelastic model. To obtain the part deformation after ejection, they used a linear elastic three-dimensional finite element approach. The results were compared with the experimental data given in [1].

Chen *et al.* [15] used a thermo-viscoelastic model to obtain the governing mathematical model of the residual stresses for amorphous polymers using a finite difference method.

Young and Wang [16] used a thermoviscoelastic model for calculation of residual stresses during postfilling stage. The temperature and pressure histories obtained from the simulation were used in their calculation of the in-mold residual stresses. The resulted in-mold stress fields were used to calculate the part warpage after demolding.

Shen and Li [17] predicted the warpage of a plastic part by finite element method based on the calculation of residual stresses developed during the molding process. In order to model the mechanism of the part warpage, they analyzed the solidification of a molten thermoplastic between cooled parallel plates.

Young [18] determined the temperature and pressure histories in the postfilling stage of the injection molding process. He calculated the developed residual stress field based on these histories, together with a simple thermoviscoelastic model. The residual stresses were then compared with the experimental data measured by Zoetelife *et al.* [1] for a plate.

Wang and Young [19] numerically investigated the effects of the process conditions on the residual stresses of a thin-walled part using elastic and viscoelastic models. They used a layer removal method to experimentally measure the residual stresses and compared them with the numerical results.

Kim *et al.* [20] predicted residual stresses in their study by numerical methods using "MoldflowTM" and "AbaqusTM". They measured residual stresses experimentally by two methods — the layer removal and hole drilling method. Then residual stress distribution predicted by the thermal stress analysis was compared with the experimental results obtained by these two methods.

A literature review indicates a shortage of study and investigation on the constrained shrinkage. Although it is well known that shrinkage of constrained dimensions is different (lower) than that of free shrinkage, further

scientific and engineering explorations are required to investigate this phenomenon.

This paper presents a numerical simulation considering of residual stresses to predict constrained shrinkage and its interrelationship with the processing parameters, here the cooling time. A rectangular plate with two square holes (as constraints) was used as the case study. The temperature and pressure distributions obtained from flow field equations of injection molding process were used to calculate the in-mold stress field. The model of in-mold residual stresses given by Young and Wang [16] were applied. Their model divides the thickness into two regions, liquid and solid phases. Residual stress calculation is just applied for the solid phase, but for liquid phase the packing pressure is applied without any strain. After demolding an elastic model is assumed to calculate the shrinkage. The numerical results are then compared with the experimental data.

FORMULATION

Flow formulation

In injection molding, plastic parts are assumed to be three-dimensional with thin-walled geometry. The polymer melt flow is assumed to be a quasi-steady flow of generalized-Newtonian compressible fluid under non-isothermal conditions. The governing equations, describing the continuity, momentum, and energy of the flow field are as follows, respectively [22]:

$$\frac{\partial \rho}{\partial t} + \frac{\partial(\rho u)}{\partial x} + \frac{\partial(\rho v)}{\partial y} = 0 \quad (1)$$

$$-\frac{\partial p}{\partial x} + \frac{\partial}{\partial z} \left(\eta \frac{\partial u}{\partial z} \right) = 0 \quad (2a)$$

$$-\frac{\partial p}{\partial y} + \frac{\partial}{\partial z} \left(\eta \frac{\partial v}{\partial z} \right) = 0 \quad (2b)$$

$$\frac{\partial p}{\partial z} = 0 \quad (2c)$$

$$\rho c_p \left(\frac{\partial T}{\partial t} + u \frac{\partial T}{\partial x} + v \frac{\partial T}{\partial y} \right) = \frac{\partial}{\partial z} \left(k \frac{\partial T}{\partial z} \right) + \beta T \frac{\partial P}{\partial t} + \eta \Theta \quad (3)$$

where: P — pressure, T — temperature, u and v — planar velocity components, ρ — polymer density, β — coefficient of thermal expansion, η — viscosity, Θ — dissipation function, k — thermal conductivity, c_p — specific heat.

Temperature and pressure histories of mold cavity can be determined using the above equations.

A cross-WLF model is used to model the viscosity [18, 21]:

$$\eta = \frac{\eta_0}{1 + \left[\eta_0 \dot{\gamma} / \tau^* \right]^{1-n}} \quad (4)$$

where: η_0 — zero shear rate viscosity, $\dot{\gamma}$ — shear rate, n — power-law index, τ^* — material constant.

Zero shear rate viscosity can be represented by a WLF-type equation as follows [16, 18]:

$$\eta_0 = D_1 \exp \left[- \frac{A_1 (T - T^*)}{A_2 + (T - T^*)} \right] \quad (5)$$

in which:

$$T^* = D_2 + D_3 P \quad (6)$$

$$A_2 = \tilde{A}_2 + D_3 P \quad (7)$$

where: D_1, D_2, D_3, A_1 and \tilde{A}_2 — material constants.

For polymer density calculation a modified two-domain Tait model is used as follow [22]:

$$V(T, P) = V_0(T) \left[1 - C \ln \left(1 + \frac{P}{B(T)} \right) \right] + V_f(T, P) \quad (8)$$

where: $V(T, P)$ — specific volume at temperature T and pressure P , V_0 — specific volume at zero gauge pressure, T — temperature (in K), P — pressure (in Pa), C — constant (0.0894), $B(T)$ — accounts for the pressure sensitivity of the material, $V_f(T, P)$ — an additional transition function required for non-amorphous (crystalline) materials.

For the analysis of residual stresses, only the packing and cooling stages of injection molding were considered. However, the analyses of the temperature and pressure fields in the filling stage are also required to obtain the initial field of the packing stage. Thus, simulations of all stages of injection molding process are used to calculate the pressure and temperature fields. During packing and cooling stages, the pressure over the liquid region in the cavity was considered equal to the packing pressure.

Residual stress analysis

The residual stress analysis of Young and Wang [16] was applied for the following stress analysis. The shear stresses are neglected in the analysis of the in-mold residual stresses. The considered stresses are the three normal stresses. The normal stress, σ_{zz} , is assumed to be constant in the thickness direction. For an isotropic material by denoting \bar{s} and s_{ij} as the spherical and deviatoric components of the stress tensor and \bar{e} and e_{ij} as the spherical and deviatoric components of the strain tensor respectively, the equations for the deviatoric stress and (spherical) bulk stress are [16, 17]:

$$s_{ij} = \int_0^t G_1(\xi - \xi') \frac{\partial e_{ij}}{\partial t'} dt' \quad (9)$$

$$\bar{s} = \int_0^t G_2(\xi - \xi') \frac{\partial (\bar{e} - e_{th})}{\partial t'} dt' \quad (10)$$

in which: G_1 and G_2 — relaxation functions for shear and dilatation, respectively, and e_{th} — thermal strain defined as follows:

$$e_{th} = \int_{T_0}^{T_1} \beta(t) dT \quad (11)$$

In equation (9) and (10), ξ is modified time-scale which, at a given point and time t , is given by [23]:

$$\xi(x_i, t) = \int_0^t \Phi[T(x_i, t')] dt' \quad (12)$$

where: Φ — shift function that is often characterized by WLF equation as follows [18, 21]:

$$\log \Phi = \frac{c_1(T - T_r)}{c_2 + T - T_r} \quad (13)$$

in which: c_1 and c_2 — material constants, T_r — the reference temperature.

The relaxation modulus of equations (9) and (10) (G_1 and G_2) are described by the following models [23]:

$$G_1(t) = \frac{E}{1+\nu} \varphi(t) = 2\mu\varphi(t) \quad (14)$$

$$G_2(t) = \frac{E}{1-2\nu} \varphi(t) = 3\kappa\varphi(t)$$

where: E — Young's modulus, ν — Poisson's ratio, μ — shear modulus, κ — bulk modulus, $\varphi(t)$ — written as follows [23]:

$$\varphi(t) = \sum_{r=1}^m g_r \exp\left(-\frac{t}{\theta_r}\right) \quad (15)$$

in which: θ_r — relaxation times and g_r — material constants.

With simplification of equations (9) and (10), the normal stresses can be written as [16]:

$$\sigma_{xx} = \sigma_{yy} = \int_0^t \varphi(\xi - \xi') \left[\left(-\frac{2\mu}{3} + \kappa \right) d\varepsilon_{zz} - 3\kappa\Delta e_{th} \right] \quad (16)$$

$$\sigma_{zz} = \int_0^t \varphi(\xi - \xi') \left[\left(\frac{4\mu}{3} + \kappa \right) d\varepsilon_{zz} - 3\kappa\Delta e_{th} \right] \quad (17)$$

Solidification of molded part and analysis of residual stresses can be separated into the three following steps [16]:

1. The core region is still in liquid phase.
2. The entire layers all solidified and the material does not detach from the mold wall.
3. The material detached from the mold wall.

For step 1., by time discretisation of Equations (16) and (17), between instant $t = t^n$ and $t = t^{n+1}$, and assuming that variation of pressure in z direction equalizes the variation of local melt pressure, the stresses are obtained as:

$$\Delta\sigma_{xx}^n = \Delta\sigma_{yy}^n = (\varphi(\Delta\xi^n) - 1) \sigma_{xx}^n + \alpha \left[(\Delta p^n - (\varphi(\Delta\xi^n) - 1) p^n) + \Gamma(\Delta\xi^n)(\varepsilon - 1)3\kappa\Delta e_{th}^n \right] \quad (18)$$

with:

$$\sigma^{n+1} = \sigma^n + \Delta\sigma^n \quad (19a)$$

$$\Gamma(\Delta\xi^n) = \sum_r \frac{g_r \left(1 - e^{-\xi/\theta_r} \right)}{\Delta\xi^n / \theta_r} \quad (19b)$$

and

$$\alpha = \frac{\left(-\frac{2\mu}{3} + \kappa \right)}{\left(\frac{4\mu}{3} + \kappa \right)} \quad (19c)$$

For the second step, applying the boundary condition of no displacement in the thickness direction (Δh_z), the variation of in-plane stress becomes:

$$\Delta\sigma_{zz}^n = \frac{\sum_{i=1}^{n_l} \frac{\Delta z_i}{\Gamma(\Delta\xi^n)} \left[\frac{\varphi(\Delta\xi^n) - 1}{\Gamma(\Delta\xi^n)} \sigma_{zz}^n - 3\kappa \Gamma(\Delta\xi^n) \Delta e_{th}^n \right]}{\sum_{i=1}^{n_l} \frac{\Delta z_i}{\Gamma(\Delta\xi^n)}} \quad (20)$$

and

$$\Delta\sigma_{xx}^n = \Delta\sigma_{yy}^n = (\varphi(\Delta\xi^n) - 1) \sigma_{xx}^n + \alpha \left[\Delta\sigma_{zz}^n - (\varphi(\Delta\xi^n) - 1) \sigma_{zz}^n \right] + \Gamma(\Delta\xi^n)(\alpha - 1)3\kappa\Delta e_{th}^n \quad (21)$$

In the third step, as the material cools further, the compressive stress in the thickness direction drops to zero, and therefore, by applying this condition ($\sigma_{zz} = \Delta\sigma_{zz} = 0$), the variation of in-plane stress becomes:

$$\Delta\sigma_{xx}^n = \Delta\sigma_{yy}^n = (\varphi(\Delta\xi^n) - 1) \sigma_{xx}^n + \Gamma(\Delta\xi^n)(\alpha - 1)3\kappa\Delta e_{th}^n \quad (22)$$

SHRINKAGE ANALYSIS

Shrinkage is prevented to occur at in-mold stage especially in the presence of constraints, thus an internal stress is induced. Because of the viscoelastic properties of plastic material and influence of cooling time, the effect is considerable. The long in-mold period signifies in-mold constraint effect, and consequently, reduces shrinkage. On the other hand, the short in-mold period reduces the in-mold constraint effect, and consequently larger shrinkage is resulted due to the released stress and the thermal contraction at the ambient conditions. In summary the final shrinkage becomes smaller as the cooling time becomes longer, and *vice versa*. Hence the influence of in-mold constraint on the final shrinkage is different depending on the duration of in-mold stage or cooling time. The calculation of shrinkage is then divided into two steps.

In-mold State

The first step is related to the mold-constraint effect where the apparent shrinkage is null, but due to the residual stress induced during postfilling stage, a certain amount of strain (shrinkage) is released at part ejection. Obviously, the amount of released strain (ε_{res}) depends on the amount of the residual stress just before ejection (σ_{eject}). This, in turn, depends on the specific relaxation time constant. If the relaxation time is small, the residual stress is low or no residual stress is preserved, and thus, material behaves more like perfect-viscous fluid. If the relaxation time is large, the residual stress is considerable and the material behaves like a perfect elastic material. In this study, after demolding, the polymer was assumed to behave as a linear elastic material. The amounts of the released strains (ε_{res}) in three directions are then obtained from the following equations:

$$\varepsilon_{xx} = \frac{1}{E} [\sigma_{xx} - \nu(\sigma_{yy} + \sigma_{zz})] \quad (23)$$

$$\varepsilon_{yy} = \frac{1}{E} [\sigma_{yy} - \nu(\sigma_{xx} + \sigma_{zz})] \quad (24)$$

$$\varepsilon_{zz} = \frac{1}{E} [\sigma_{zz} - \nu(\sigma_{xx} + \sigma_{yy})] \quad (25)$$

Out of mold state

At the second step, the amount of thermal shrinkage (ϵ_{th}) is calculated which corresponds to the difference between the temperature of the part at ejection (T_{eject}) and the ambient temperature (T_{amb}). The amount of the thermal shrinkage (thermal strain ϵ_{th}) can be obtained as follows:

$$\epsilon_{th} = \int_{T_{eject}}^{T_{amb}} \beta(t) dT \quad (26)$$

Total shrinkage (ϵ_{total}) then becomes the sum of the two above shrinkages:

$$\epsilon_{total} = \epsilon_{res} + \epsilon_{th} \quad (27)$$

A finite volume method was used to compute the residual stress in the postfilling stage. In order to investigate the interrelationship among the constraint feature and cooling time, a numerical simulation was developed for a simple geometry with constraint (a rectangular plate with of two square holes). The purpose was to predict the variation of final dimension (or final shrinkage) of the square holes *versus* cooling time.

RESULTS AND DISCUSSION

As the initial step the simulation results were compared with the available numerical and experimental data given by other researchers. The example was a flat plate model used by Zoetelife *et al.* [1] as shown in Figure 1. The plate was a rectangular strip (300×75×2.5) molded of acrylonitrile-butadiene-styrene (ABS, “Novodur P2X” of Bayer). The melt temperature, mold temperature, injection rate and packing pressure were 240 °C, 48–52 °C, $1.2 \cdot 10^{-5} \text{ m}^3/\text{s}$ and 50 MPa respectively.

Figure 2 shows the experimental and calculated stress profile *versus* thickness at a position between P_2 and P_3 (see Fig. 1) and compares them with the numerical results of the present research. The three stress pro-

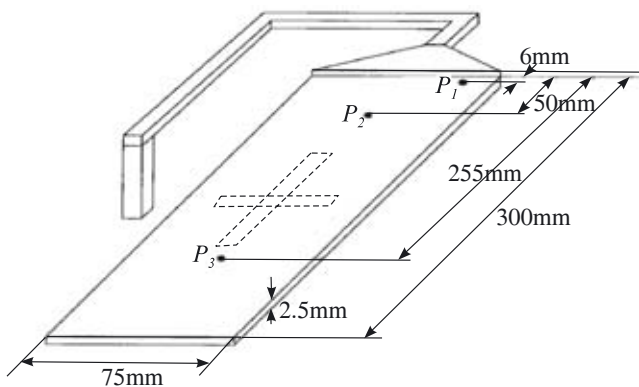


Fig. 1. Geometry of rectangular strip used in the simulation [1]

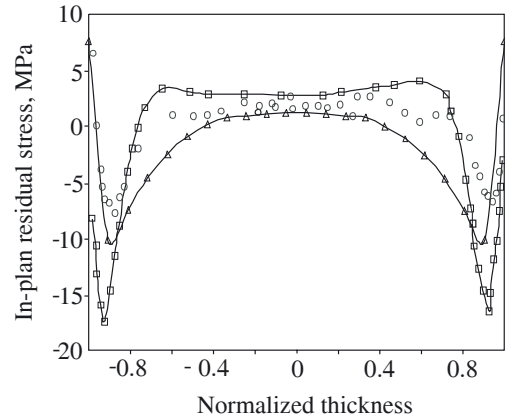


Fig. 2. Comparison of in-mold residual stress distribution results; -o- — experimental results of Zoetelife *et al.* [1], -□- — numerical results of Zoetelife *et al.* [1], -Δ- — present study results

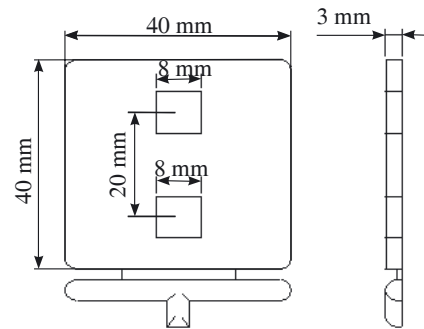


Fig. 3. Film-gated molded part used in the simulation

files introduce similar features: tensile stress at the surface, compressive stress at the sub-surface, and again tensile stress in the core of a sample. Figure 2 also shows a good agreement between [1] and the present results, following the distribution trend of the previous study.

In the present research, aiming for the prediction of the in-mold constrained shrinkage, a rectangular plate (dimensions 40 mm×40 mm×3 mm) with two square holes of dimension 8 mm (as constraints) was used (Fig. 3). As mentioned before, the purpose was to predict the variation of final dimension (or final shrinkage) of the holes *versus* cooling time.

Acrylonitrile-butadiene-styrene (ABS, “Novodur P2H-AT” of Bayer) was used as the experimental material according to the specifications listed in Table 1–4. The processing parameters are given in Table 5.

Table 1. Material specification of ABS used [1, 24]

Material data	Symbol	Value
Specific heat	c_p	1800 J/(kg · K)
Thermal conductivity	k	0.127 W/(m · K)
Elastic modulus	E	2.24 GPa
Poisson’s ratio	ν	0.392

Table 2. Constants for Tait equation (8) for ABS used [1, 24]

Constant	Value	Unit
b_{11}	$9.73 \cdot 10^{-4}$	m^3/kg
b_{21}	$5.60 \cdot 10^{-7}$	$\text{m}^3/\text{kg} \cdot \text{K}$
b_{31}	$2.61 \cdot 10^8$	Pa
b_{41}	$3.90 \cdot 10^{-3}$	1/K
b_{1m}	$9.73 \cdot 10^{-4}$	m^3/kg
b_{2m}	$2.27 \cdot 10^{-7}$	$\text{m}^3/\text{kg} \cdot \text{K}$
b_{3m}	$3.05 \cdot 10^8$	Pa
b_{4m}	$4.10 \cdot 10^{-3}$	1/K
b_5	363	K
b_6	$1.47 \cdot 10^{-7}$	K/Pa
b_7	0	m^3/kg
b_8	0	1/K
b_9	0	1/Pa

Table 3. Constants for cross-WLF model for ABS used [1, 24]

Constant	Value	Unit
N	0.3489	m^3/kg
τ^*	52 400	$\text{m}^3/(\text{kg} \cdot \text{K})$
D_1	$2.84 \cdot 10^2$	Pa
D_2	$3.90 \cdot 10^{-3}$	1/K
D_3	$9.73 \cdot 10^{-4}$	m^3/kg
A_1	$2.27 \cdot 10^{-7}$	$\text{m}^3/(\text{kg} \cdot \text{K})$
A_2	$3.05 \cdot 10^8$	Pa

Table 4. Relaxation data (6-mode relaxation spectrum) for ABS used [1]

i	θ_i (s)	G_i (Pa)
1	$4.706 \cdot 10^{-9}$	$5.074 \cdot 10^7$
2	$4.410 \cdot 10^{-6}$	$8.688 \cdot 10^7$
3	$2.082 \cdot 10^{-3}$	$2.904 \cdot 10^8$
4	$9.198 \cdot 10^{-1}$	$4.091 \cdot 10^8$
5	$3.035 \cdot 10^6$	$3.573 \cdot 10^5$
6	$2.749 \cdot 10^8$	$1.185 \cdot 10^5$

Table 5. Processing parameters used in the injection molding experiments

Processing parameters	Symbol	Value
Melt temperature	T_m	250 °C
Mold temperature	T_w	50 °C
Injection time	t_{in}	1.5 s
Packing pressure	P_h	60 MPa
Packing time	t_h	12 s

Figure 4 shows the in-plane residual stress distribution obtained from the numerical simulation in the present study. The residual stress profiles are given at different times of cooling and along a-a section, *versus* the sample thickness and crossing the middle point of the part, as shown in Fig. 5. The stress profile is similar to the previous example with tension at the surface and the core regions and compression at subsurface. In Fig. 6 the residual stress profile along b-b section of Figure 5 for different times of cooling is shown. This section is again crossing the middle point of the part, but it is along the length of the part. It can be seen that the obtained resi-

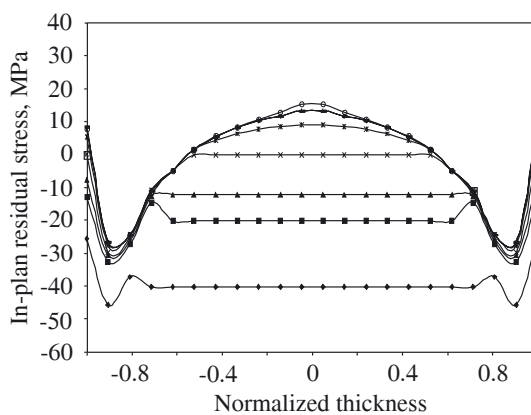


Fig. 4. Variation of in-mold residual stress as the function of sample thickness (a-a, section, see Fig. 5); time of cooling (s): -◆- 5, -■- 10, -▲- 12, -×- 13,5, -* 15, -o- 18, -/ 23, --- 26, --- 30

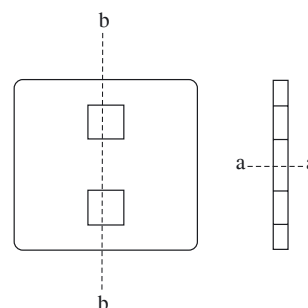


Fig. 5. Sections of the part selected to show the stress data

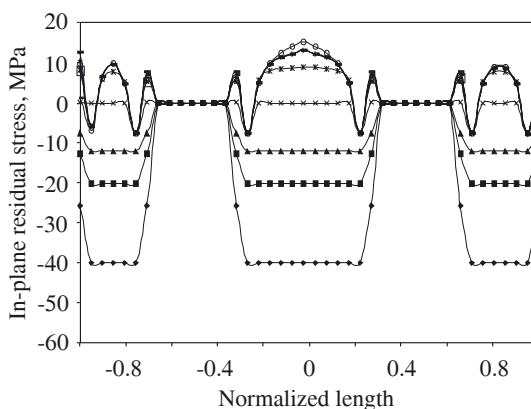


Fig. 6. Variation of in-mold residual stress as the function of sample length and at the middle (b-b, section); time of cooling (s) see Fig. 4

dual stress profile between every two walls of the part is similar to the two previous examples. As Figure 6 shows, the calculated residual stresses at the left side of the part are slightly higher than the right side ones. This could be due to the effect of the gate system that may cause a slightly lower cooling rate close to the gate area (left side of the part).

To examine the numerical prediction of the constrained shrinkage, a specific experimental work was conducted as follows. A 70-ton "POOLAD" injection

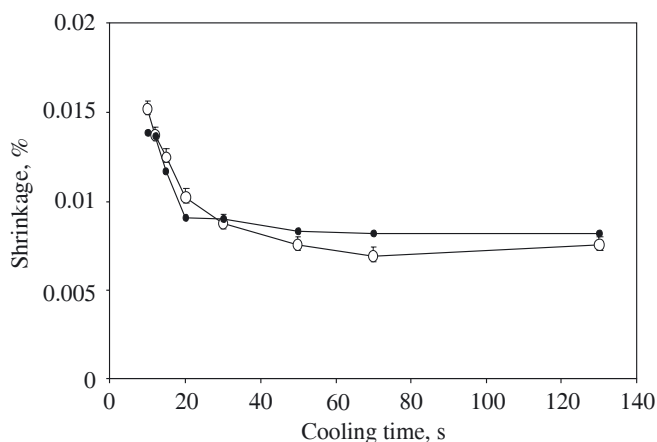


Fig. 7. Comparison of the shrinkage predicted from the numerical analysis (●) and the experimental data (○, average of two holes)

machine was used to produce the specimens. The initial experimental conditions are set to match the numerical analysis. To achieve different cooling time values, appropriate setting was carried out. The cooling times, before ejection, were 10, 12, 15, 20, 30, 50, 70 or 130 s. At least, three experiments were produced for each test point to obtain credible results and the conditions of molding were maintained steady. The measured shrinkage is calculated as following:

$$\% \text{ shrinkage} = \frac{d - d_0}{d_0} \cdot 100 \quad (28)$$

where: d — the final dimension, d_0 — the dimension of insert (producing hole).

Figure 7 presents the shrinkage data obtained from the numerical analysis and experimental results, at various cooling times. It can be seen, that there is a good agreement between these values. They indicate that the numerical simulation developed in this study explains the constrained shrinkage with an acceptable degree of accuracy. The difference between experimental and computational results could be due to the combination of measurement errors in experiments and the calculated shrinkage which has been obtained by completely converting the residual stresses into shrinkage (in contrast, some residual stress may still reside in the part).

CONCLUSION

A numerical simulation was developed, considering the residual stresses, in order to predict constrained shrinkage. The temperature and pressure fields from the simulation of the injection stages were used in the calculations of residual stresses. Investigation of the relationship between the shrinkage value and the processing parameter (cooling time) in a viscoelastic amorphous material (ABS) was carried out. The developed numerical analysis was then experimentally examined using a case study, namely, a rectangular plate with two square holes (as constraints). The results let conclude that:

— there is a good agreement between the numerical and experimental data;

— cooling time has a significant effect on the final shrinkage of a constrained feature, especially at a low cooling time value; above a certain cooling time value, the change in dimension is insignificant.

ACKNOWLEDGMENT

The authors would like to thank Germany Bayer Co. for preparing ABS material, and Mr. H. Motabar and Iranian Part Electric Company for their assistance in experimentation.

REFERENCES

1. Zoetelief W. F., Douven L. F. A., Ingen Housz A. J.: *Polym. Eng. Sci.* 1996, **36**, 19.
2. Williams R. F., Pacoast L. H.: *Mod. Plast. Int.* 1967, 185.
3. Mamat A., Trochu F., Sanschagrín B.: *Polym. Eng. Sci.* 1995, **35**, 19.
4. Leo V., Cuvellez C.: *Polym. Eng. Sci.* 1996, **36**, 15.
5. Young W. B.: *Int. Polym. Process.* 2000, 416.
6. Chang R. Y., Chang W. Y., Yang W. H.: *SPE ANTEC Tech.* 2001, paper 736.
7. Xu H., Kazmer D. O.: *Polym. Eng. Sci.* 2001, **41**, 9.
8. Pontes A. J.: "Shrinkage and Ejection Forces in Injection Molding Products", Ph.D Thesis, University of Minho, Portugal, 2002.
9. Peng Y. H., Hsu D. C., Yang V.: *SPE ANTEC Tech.* 2004, p. 524.
10. Postawa P.: *Polimery* 2005, **50**, 201.
11. Chen C. C. A., Tzeng S. L., Kao S. C.: 22nd Annual Meeting of the Polymer Processing Society, Yamagata, Japan, 2006, mat. konf. G08-06.
12. Kowalska B.: *Polimery* 2007, **52**, 280.
13. Boitout F., Agassant J. F., Vincent M.: *Int. Polym. Process.* 1995, 237.
14. Choi D. S., Im Y. T.: *Compos. Struct.* 1999, **47**, 655.
15. Chen X., Lam Y. C., Li D. O.: *J. Mat. Proc. Technol.* 2000, **101**, 275.
16. Young W. B., Wang J.: *Int. Polym. Process.* 2002, 271.
17. Shen C. Y., Li H. M.: *Polym. Plast. Technol. Eng.* 2002, **42**, 5.
18. Young W. B.: *J. Process. Technol.* 2004, **45**, 317.
19. Wang T. H., Young W. B.: *Eur. Polym. J.* 2005, **41**, 2511.
20. Kim S., Kim C., Oh H., Youn J. R.: 22nd Annual Meeting of the Polymer Processing Society, Yamagata, Japan 2006, mat. konf. G08-13.
21. Kennedy P.: "Flow Analysis of Injection Molds", Hanser & Gardner Publishers, New York, 1995.
22. Chang R. Y., Chen C. H., Su K. S.: *Polym. Eng. Sci.* 1996, **36**, 1789.
23. Kabanemi K. K., Vaillancourt H., Wang H., Salloum G.: *Polym. Eng. Sci.* 1998, **38**, 21.
24. Moldflow Co., Technical Data, Moldflow Plastics Insight, 1998.

Received 7 II 2007.